
Demonstration of the effectiveness and limitations of thin airfoil theory in the aerodynamic study of airfoil characteristics

N. A. Ahmed

Associate Professor in Aerospace Engineering, School of Mechanical and Manufacturing Engineering, University of New South Wales, Sydney, NSW 2052, Australia
E-mail: n.ahmed@unsw.edu.au

Abstract Aerodynamics as a branch of science is based on many idealized concepts and ingenious abstractions and approximations. The teaching of aerodynamics, in this context, becomes a challenging undertaking. In order to demonstrate the relevance of these concepts to real situations, it is important that appropriate experimental demonstrations are devised. In this paper we describe such an experimental programme to demonstrate the usefulness and limitations of thin airfoil theory in the analysis of the aerodynamic characteristics of an airfoil. This programme is easy to implement and has been incorporated in the teaching of aerodynamics to undergraduate students at the University of New South Wales.

Keywords airfoil, aerodynamic characteristics, thin airfoil theory.

Notation

| | |
|-------------------------------|---|
| A_0, A_1, \dots, A_n | coefficients associated with vortex strength |
| c | cord length |
| C_D | form drag coefficient |
| C_P | pressure coefficient |
| C_L | lift coefficient |
| C_N, C_T | normal and tangential force coefficients |
| $C_{M_{L.E.}}, C_{M_{0.25c}}$ | moment coefficients about leading edge and quarter cord |
| L | lift per unit span |
| p | static pressure measured at any tapping position |
| p_T | free stream total pressure |
| p_8 | free stream static pressure |
| $\Delta p = p - p_\infty$ | static pressure change on the airfoil with reference to free stream |
| $q_\infty (= p_T - p_\infty)$ | dynamic head of free stream |
| θ | angular representation of location of a point on mean camber line |
| R_e | Reynolds number, based on cord length |
| U_∞ | free stream velocity |
| x, y | Cartesian coordinates |
| y_l, y_u | lower and upper vertical distance |
| ρ_∞ | density of free stream |
| G | circulation |
| Γ | vortex strength |
| γ | vortex strength per unit length |

Introduction

'Aerodynamics is a subject of intellectual beauty, composed and drawn by many great minds over the centuries' [1, p. xvi]. The flight of man and the exploration of space would not have been possible without great advances in aerodynamics. In spite of this, even today, aerodynamicists work very close to the frontier between 'bewilderment and understanding' [2, p. 2]. Aerodynamics as a branch of science has prospered on highly idealized concepts and ingenious abstractions and approximations, and has become a study not only of facts but also of indulgence in fancies. According to Kuchemann [2, p. 23], 'many of the concepts in current use are really personal views on the matter, put forward by some individual scientists or some school of scientists or engineers and then more generally adopted'. The application of aerodynamics to any successful design of aircraft or any other fluid mechanical device requires, therefore, more than anything else, imagination and initiative in speculations and conjectures, followed by comprehensive testing of the design concepts employed.

The teaching of aerodynamics to undergraduate students, in this context, becomes a challenging undertaking. The whole process can, however, be fun and rewarding if the students are taken on a journey where, en route, they begin to appreciate the intuitive art of those scientists to whom we owe the many useful concepts and approximations with which we work.

The purpose of the present paper is to participate in such a journey through a simple wind tunnel experiment which has been incorporated in the aerodynamics course at the University of New South Wales, Australia. In this experiment we highlight the idealized concept of thin airfoil theory and show its effectiveness and limitations when applied to real situations.

Fundamentals of thin airfoil theory

The thin airfoil theory was developed by Prandtl during World War I. It is still used today [3, p. 257] because it offers a very simple but reliable and practical method of calculating airfoil properties. The basis of the theory may be briefly described as follows. At low angles of incidence, the boundary layer growth on an airfoil is thin and remains attached to the airfoil, which allows the flow to be assumed inviscid and irrotational. Furthermore, since the thickness of any lifting airfoil is less than a fifth of its chord length, the effect of the thickness is neglected and the airfoil is represented by its mean camber line. A hypothetical or mathematically conceived function in the form of a vortex sheet is then placed along the length of the camber line to simulate the airfoil, which essentially makes it a streamline of the flow. Applying the circulation theory of lift to this streamline, the aerodynamic properties of the airfoil are obtained.

Mathematically, the lift per unit span is given by [1, pp. 277–278]:

$$L = \rho_{\infty} U_{\infty} \Gamma \quad (1)$$

where

$$\Gamma = \frac{c}{2} \int_0^\pi \gamma(\theta) \sin \theta d\theta \quad (2)$$

$$\gamma(\theta) = 2U_\infty \left[A_0 \frac{(1 + \cos \theta)}{\sin \theta} + \sum_{n=1}^{\infty} A_n \sin n\theta \right] \quad (3)$$

$$A_0 = \alpha - \frac{1}{\pi} \int_0^\pi \frac{dy}{dx} d\theta \quad (4)$$

$$A_n = \frac{2}{\pi} \int_0^\pi \frac{dy}{dx} \cos n\theta d\theta \quad (5)$$

and

$$x = \frac{c}{2} (1 - \cos \theta) \quad (6)$$

It is then a simple matter to show that [1, pp. 277–278]:

$$C_L = \pi(2A_0 + A_1) \quad (7)$$

and

$$C_{M_{L.E.}} = - \left[\frac{C_L}{4} + \frac{\pi}{4} (A_1 - A_2) \right] \quad (8)$$

$$C_{M_{0.25c}} = - \left[\frac{\pi}{4} (A_1 - A_2) \right] \quad (9)$$

Thus a knowledge of only the geometry of the mean camber line is sufficient to produce the properties of an airfoil quite accurately. It therefore becomes a simple but powerful tool in airfoil design and analysis.

In order to investigate the effectiveness and limitation of the thin airfoil theory, students are asked to use the theory to calculate the angle of zero lift, and coefficients of lift and moment at various angles of attack for a particular airfoil. Thereafter, the students are asked participate in a wind tunnel experiment to evaluate these parameters, as well as the drag associated with the same airfoil from pressure tapping measurements on the top and bottom surfaces of the airfoil. Finally, the results by the two methods are compared with published data.

Laboratory experiment

The five-digit NACA 23012 airfoil, which is widely used in practice, was chosen for this study. An aluminium wing (6-inch cord \times 18-inch span) was manufactured

from geometrical information readily available in the literature [4, p. 413, 5, p. 7].

The wing was made of two halves joined together so that hypodermic needle tubes could be inserted and joined to the pressure tapping points. These tubes were taken out from one end of the wing and connected to a multi-tube manometer via plastic tubes in such a way as to facilitate a direct visual display on the manometer of the top and bottom surface pressure distributions for a particular angle of incidence. The other end of the wing was connected to a mechanical arrangement outside the tunnel to set the wing at different angles of incidence. Details of the pressure tapping locations are given in Fig. 1 and Table 1. Also, to avoid any wall effect, the pressure tapping points were located at mid-span of the wing. A Pitot static tube and a Betz manometer were used to record wind tunnel airspeed upstream of the airfoil.

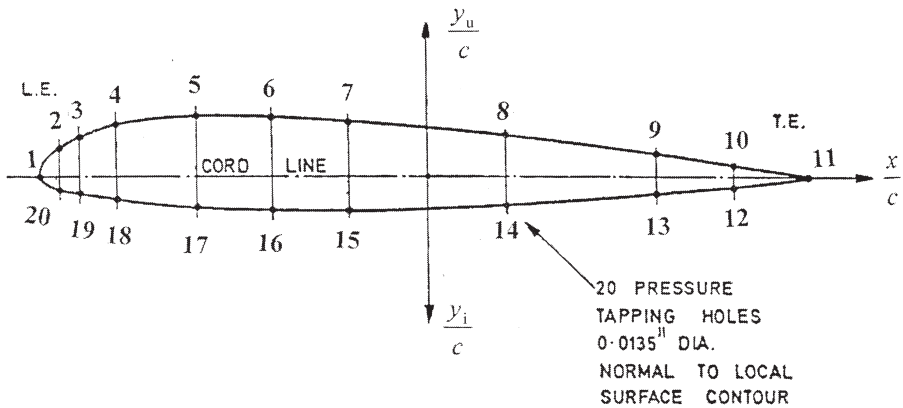


Fig. 1 Pressure tapping locations on the NACA 23012 airfoil.

TABLE 1 Coordinates of tapping point locations shown in Fig. 1

| Pressure tapping location | Cord-wise distance (%): $\frac{x}{c}$ | Distance above cord line (%): $\frac{y_u}{c}$ | Distance below cord line (%): $\frac{y_i}{c}$ | Thickness – cord ratio (%): $\frac{t}{c}$ |
|---------------------------|---------------------------------------|---|---|---|
| 1 | 0 | 0 | 0 | 0 |
| 2, 20 | 2.5 | 3.61 | -1.71 | 5.32 |
| 3, 19 | 5.0 | 4.91 | -2.26 | 7.17 |
| 4, 18 | 10.0 | 6.43 | -2.92 | 9.35 |
| 5, 17 | 20.0 | 7.50 | -3.97 | 11.47 |
| 6, 16 | 30.0 | 7.55 | -4.46 | 12.01 |
| 7, 15 | 40.0 | 7.14 | -4.48 | 11.62 |
| 8, 14 | 60.0 | 5.47 | -3.67 | 9.14 |
| 9, 13 | 80.0 | 3.08 | -2.40 | 5.24 |
| 10, 12 | 90.0 | 1.68 | -1.23 | 2.91 |
| 11 | 100.0 | 0.13 | -0.13 | 0.26 |

The wing was placed in the test section (18 inch \times 18 inch) of the wind tunnel of the University of New South Wales in such a way that its ends were terminated by the wind tunnel walls. This way a two-dimensional flow was created on the wing.

Students were given the following instructions for the procedure and for the data reduction they were required to undertake.

Procedure

- (1) Laboratory staff will prepare the 18-inch square wind tunnel and 6-inch cord NACA 23012 airfoil and instruments.
- (2) A multi-tube manometer is used to read surface pressure at 20 locations around the airfoil as shown in Fig. 1.
- (3) Use a protractor against the cord line to read airfoil incidence.
- (4) Select a suitable test section air speed after inspecting the range of movement of the manometer liquid through a complete cycle of incidence – negative stall to positive stall.
- (5) At each of several values of incidence (say, every 2 degrees centred on 0 degrees, and positive and negative stall) record the wind speed pressure reading and airfoil surface pressure readings.

Data reduction

- (1) Calculate C_p at each static pressure tap for each incidence and enter in a single table.
- (2) Plot C_p distribution against both $\frac{x}{c}$ and $\frac{y}{c}$.
- (3) Plot $(C_p \cdot \frac{x}{c})$ distribution against $\frac{x}{c}$.
- (4) Graphically evaluate C_N and C_T at each incidence angle (N and T denote normal and tangential directions to cord line, respectively).

Use the following formulae:

$$C_N = \oint C_p d\left(\frac{x}{c}\right) \quad (10)$$

$$C_T = \oint C_p d\left(\frac{y}{c}\right) \quad (11)$$

- (5) Calculate:

$$C_L = C_N \cos \alpha - C_T \sin \alpha \quad (12)$$

$$C_D = C_N \sin \alpha + C_T \cos \alpha \quad (13)$$

- (6) Graphically evaluate:

$$C_{M.L.E.} = -\oint C_p \left(\frac{x}{c}\right) d\left(\frac{x}{c}\right) \quad (14)$$

$$C_{M_{0.25c}} = C_{M_{L.E.}} + \frac{C_L}{4} \tag{15}$$

- (7) Plot C_L , C_D and $C_{M_{L.E.}}$ against angle of incidence, α .
- (8) Determine $\alpha_{L=0}$.
- (9) Determine R_{e_c} .
- (10) Compare airfoil characteristics with thin airfoil theory results and other published data.
- (11) Comment on the validity of your results.

Results

The values for C_L and $C_{M_{L.E.}}$ obtained from thin airfoil theory, a typical laboratory experiment conducted at the aerodynamics laboratory (at $R_e = 3.15 \times 10^5$) at the University of New South Wales and the data (at $R_e = 6 \times 10^6$ and standard roughness) of Abbott and Von Doenharn [4, pp. 498–499] for the NACA 23012 airfoil were plotted against α . However, the C_D values were plotted against C_L . The resulting curves are shown in Figs 2–4.

For illustrative purposes, sample calculations are given below, from thin airfoil theory for the NACA 23012 airfoil set at 5 degrees angle of incidence, followed by the reduction of the results from the laboratory experiment for the airfoil set at the same angle of incidence.

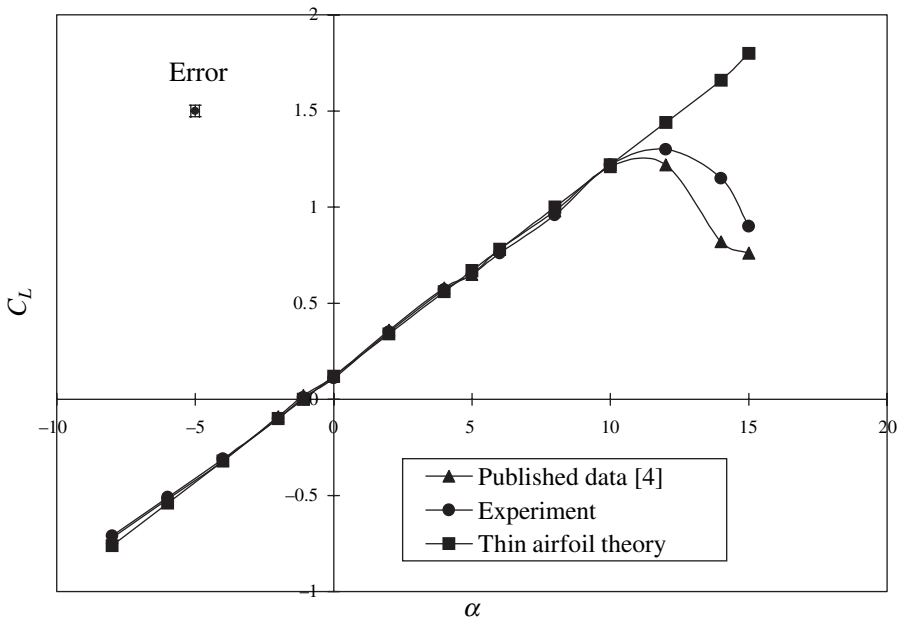


Fig. 2 Aerodynamic properties of NACA 23012 airfoil: C_L vs α .

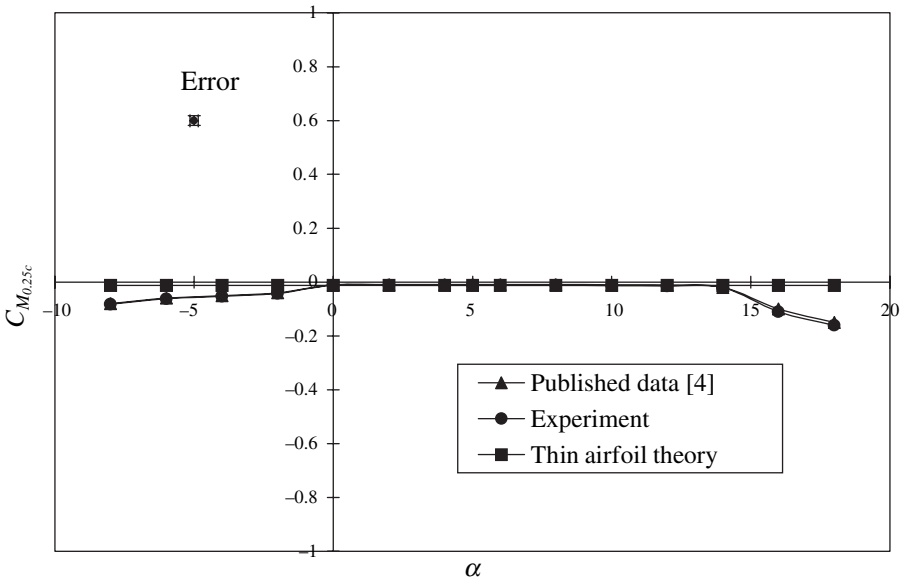


Fig. 3 Aerodynamic properties of NACA 23012 airfoil: $C_{M_{0.25c}}$ vs α .

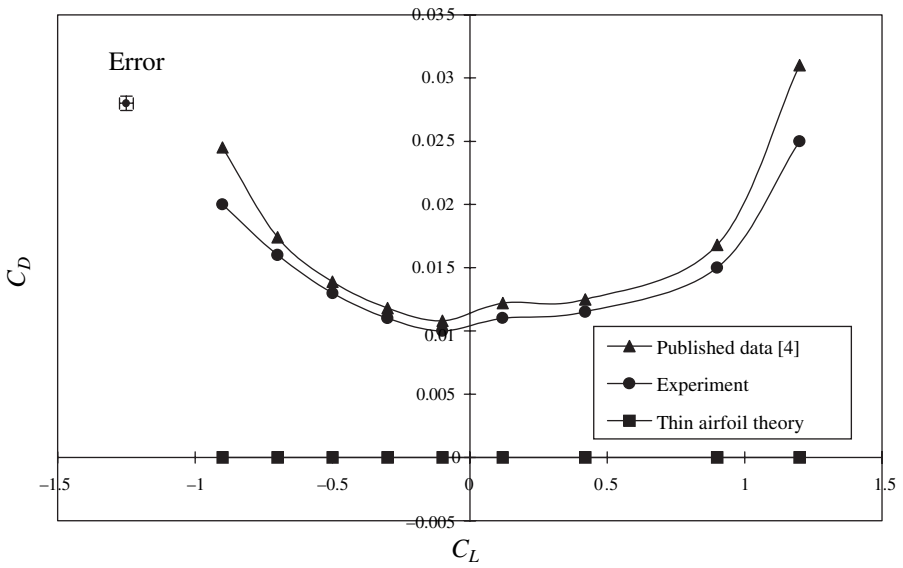


Fig. 4 Aerodynamic properties of NACA 23012 airfoil: C_D vs C_L .

Sample theoretical calculations

From [5], the mean camber line of NACA 23012 can be described by:

$$\frac{y}{c} = A\left(\frac{x}{c}\right)^3 + B\left(\frac{x}{c}\right)^2 + C\left(\frac{x}{c}\right) + D \quad \text{for } 0 \leq \frac{x}{c} \leq L$$

$$\frac{y}{c} = E\left(1 - \frac{x}{c}\right) \quad \text{for } L \leq \frac{x}{c} \leq 1 \quad (16)$$

where $A = 2.6595$; $B = -1.6156$; $C = 0.3051$; $D = 0$; $E = 0.2208$ and $L = 0.2025$.

Differentiating with respect to x :

$$\frac{dy}{dx} = 3A\left(\frac{x}{c}\right)^2 + 2B\left(\frac{x}{c}\right) + C \quad \text{for } 0 \leq \frac{x}{c} \leq L$$

$$\frac{dy}{dx} = -E \quad \text{for } L \leq \frac{x}{c} \leq 1 \quad (17)$$

Using equation (6) and substituting values for the coefficients A to E and L in (17):

$$\frac{dy}{dx} = 0.6840 - 2.3736 \cos \theta + 1.995 \cos^2 \theta \quad \text{for } 0 \leq \theta \leq 0.9335,$$

$$\frac{dy}{dx} = -0.02208 \quad \text{for } 0.9335 \leq \theta \leq \pi \quad (18)$$

From equation (4), (5) and (7), the angle of zero lift:

$$\alpha_{L=0} = -\frac{1}{\pi} \int_0^{\pi} \frac{dy}{dx} (\cos \theta - 1) d\theta = -1.09^\circ = -0.019 \text{ rad} \quad (19)$$

Consequently:

$$C_L = 2\pi(\alpha - \alpha_{L=0}) = 2\pi(\alpha + 0.0191) \quad (20)$$

For $\alpha = 5$ degrees, from (20):

$$C_L = 0.67$$

$$C_{M_{L.E.}} = -\left[\frac{C_L}{4} + \frac{\pi}{4}(A_1 - A_2)\right] = -\left[\frac{C_L}{4} + 0.0127\right] \quad (21)$$

$$C_{M_{0.25c}} = -\frac{\pi}{4}(A_1 - A_2) = -0.0127 \quad (22)$$

Thus the value of $C_{M_{0.25c}}$ is calculated to be a constant and is independent of the angle of incidence.

Sample reduction of experimental data

Raw and calculated data for C_p obtained at $\alpha = 5$ degrees and $R_e = 3.15 \times 10^5$ are given in Table 2. Graphical evaluation of C_N , C_T and $C_{M_{L.E.}}$ at this angle of incidence

TABLE 2 Raw data and calculated values of C_p (at $\alpha = 5$ degrees and $q_\infty = p_T - p_\infty = 2.76$ inches)

| Pressure tapping point (see Fig. 1) | Δp as read on manometer (in inches) | $C_p = \frac{\Delta p}{q_\infty}$ |
|-------------------------------------|---|-----------------------------------|
| 1 | 2.05 | 0.74 |
| 2 | -3.68 | -1.33 |
| 3 | -3.36 | -1.22 |
| 4 | -3.11 | -1.13 |
| 5 | -2.69 | -0.97 |
| 6 | -2.19 | -0.79 |
| 7 | -1.70 | -0.62 |
| 8 | -1.06 | -0.38 |
| 9 | -0.49 | -0.18 |
| 10 | -0.21 | -0.08 |
| 11 | 0.21 | 0.08 |
| 12 | 0.14 | 0.05 |
| 13 | 0.07 | 0.07 |
| 14 | -0.14 | -0.05 |
| 15 | -0.28 | -0.07 |
| 16 | -0.21 | -0.08 |
| 17 | -0.07 | -0.03 |
| 18 | 0.42 | 0.15 |
| 19 | 1.06 | 0.38 |
| 20 | 1.56 | 0.57 |

are shown in Figs 5–7. The C_N , C_T and $C_{M_{L.E.}}$ values were found to be 0.63, -0.04 and -0.38 , respectively. Finally, using equations (12), (13) and (15), the values for C_L , C_D and $C_{M_{0.25c}}$ were obtained as 0.64, 0.015 and -0.12 , respectively.

Discussion

The C_L , C_D and $C_{M_{0.25c}}$ values for NACA 23012 at $\alpha = 5$ degrees obtained by the above two methods are compared with published data [4] in Table 3. The values of $\alpha_{L=0}$ are also included in this table which the students should obtain from the C_L versus α curve. As can be seen, the results are all in close agreement. Such deduction of experimental results in graphical form (Figs 5–7) are expected to help students observe clearly how the pressure distributions are altered at different angles of incidence, which segments contribute most to the lift production and where losses occur due to drag.

From thin airfoil theory, equation (20) suggests that a linear relationship exists between C_L and α , i.e., as α increases so does C_L and vice versa (Fig. 2). Equation (19) suggests that the theory can also predict the angle of zero lift quite accurately. Since the thin airfoil theory, in its formulation, neglects boundary layer growth on the airfoil, it cannot predict stall angle (positive or negative) and would predict a

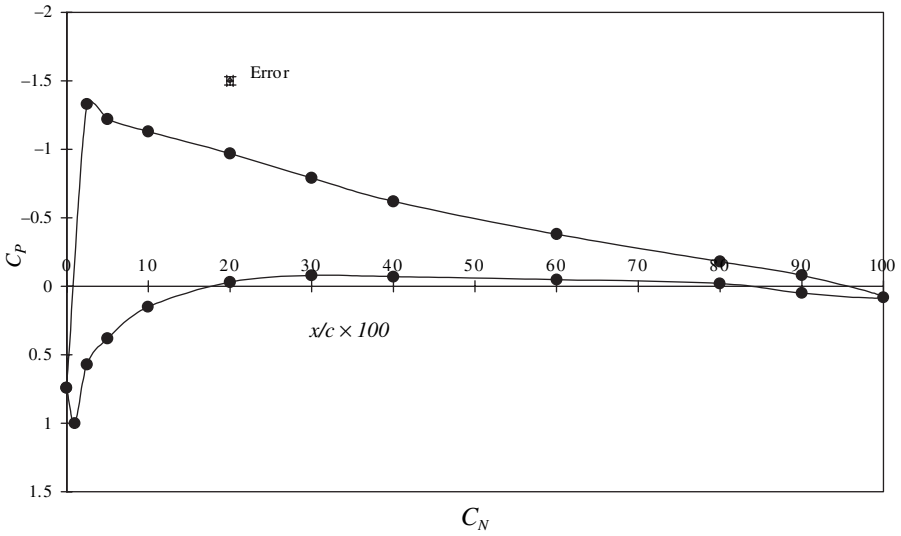


Fig. 5 Graphical determination of C_N (NACA 23012 airfoil, $\alpha = 5$ degrees, $R_e = 2.1 \times 10^5$): $C_N = \oint C_p d\left(\frac{x}{c}\right) = \text{area under curve} = 0.63$.

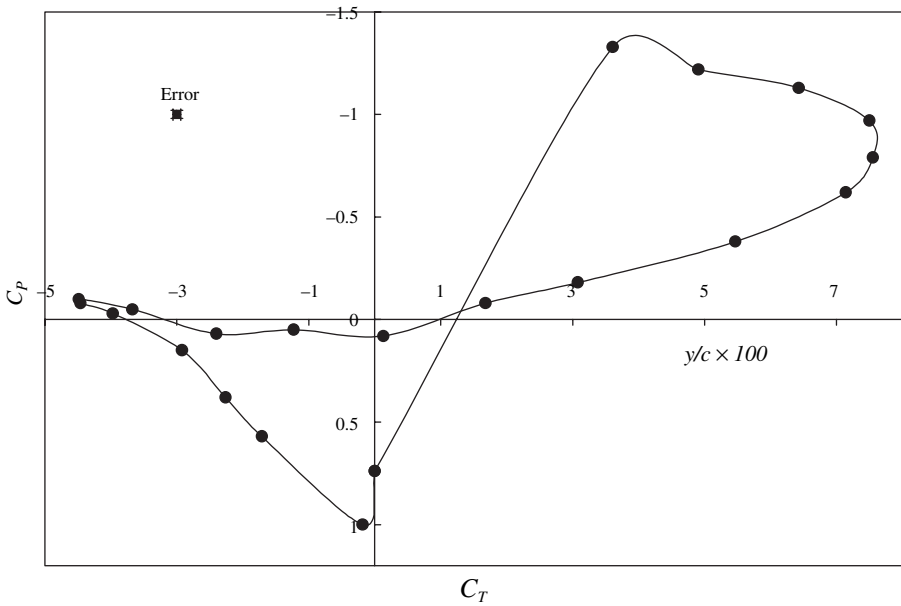


Fig. 6 Graphical determination of C_T (NACA 23012 airfoil, $\alpha = 5$ degrees, $R_e = 2.1 \times 10^5$): $C_T = \oint C_p d\left(\frac{y}{c}\right) = \text{area under curve} = -0.04$.

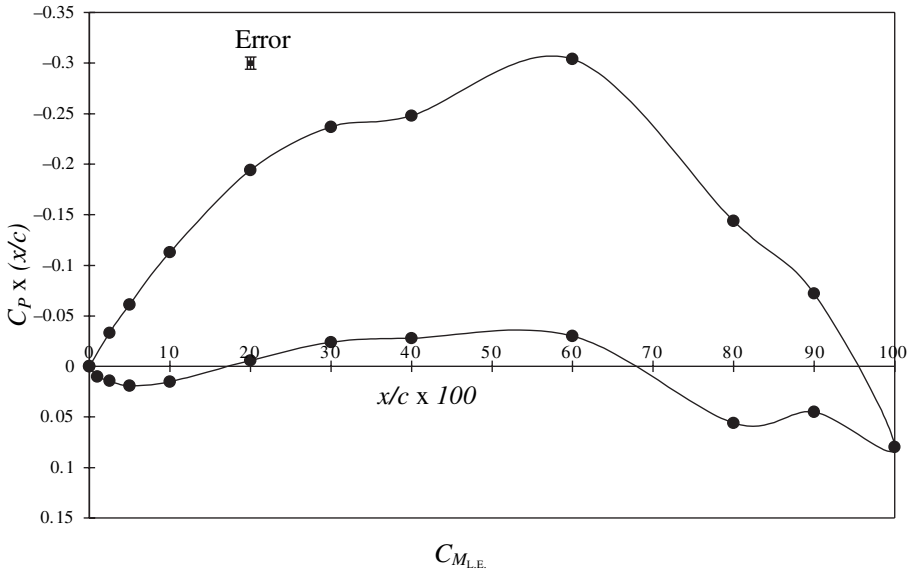


Fig. 7 Graphical determination of $C_{M_{L,E}}$ (NACA 23012 airfoil, $\alpha = 5$ degrees;

$$R_e = 2.1 \times 10^5): C_{M_{L,E}} = \oint C_p \left(\frac{x}{c} \right) d \left(\frac{x}{c} \right) = \text{area under curve} = -0.38.$$

TABLE 3 Comparison of results

| Parameter | Thin airfoil theory | Laboratory experiment | Published data [4] |
|---|---------------------|-----------------------|--------------------|
| $\alpha_{L=0}$ | -1.09 degrees | -1.1 degrees | -1.1 degrees |
| C_L at $\alpha = 5$ degrees | 0.67 | 0.64 | 0.65 |
| $C_{M_{0.25c}}$ at $\alpha = 5$ degrees | -0.13 | -0.12 | -0.11 |
| C_D at $\alpha = 5$ degrees | 0 | 0.015 | 0.014 |

zero value for C_D . In practice, however, the C_D value would be non-zero (Fig. 4). In other words, the thin airfoil theory is always expected to predict slightly higher values of C_L than are found in practice at higher angles of incidence. Students should, therefore, expect greater discrepancies between theoretical and experimental C_L values as the stall angle is approached. The greater loss in lift would, however, show up in higher C_D values from experiment. For $C_{M_{0.25c}}$ values, the thin airfoil prediction corresponds well with experiment (Fig. 3). Again, the agreement decreases as the stall angle is approached.

It is, however, worth pointing out that aircraft are designed to operate below stall angle where the results are not affected significantly by changes in the Reynolds number of the flow. Consequently, the predicted results from thin airfoil theory become very useful in the design and analysis of properties of airfoils.

Finally, it is important to realize that it is difficult to reproduce identical test conditions because it is not easy to match the roughness finish of the model, turbulence level or the Reynolds number of the flow in different experiments. Consequently, there will be some differences in experimental results. In Abbott and Von Doenham [4, pp. 498–499], experimental results for four test Reynolds numbers are given, three of which are for smooth conditions and one for standard roughness. For student laboratory experiments, the standard roughness condition is suggested since it is easier to match.

Conclusions

A detailed description of a simple teaching programme to highlight the effectiveness and limitations of thin airfoil theory has been given in this paper. The results (Figs 2–4) demonstrate that the thin airfoil theory is effective in predicting important design parameters such as the angle of zero lift or the lift and moment coefficients at various angles of incidence prior to stall. The theory has, therefore, proved beneficial for nearly a century and is still used today. It is, however, unable to predict drag, which has to be obtained by other methods, such as the one outlined in the laboratory experiment. A combination of theory and experiment should, therefore, help students understand better the various concepts associated with aerodynamic study of airfoil properties.

References

- [1] J. D. Anderson, Jr, *Fundamentals of Aerodynamics* (2nd edn) (McGraw-Hill, New York, 1991).
- [2] D. Kuchemann, *The Aerodynamic Design of Aircraft* (Pergamon Press, Oxford, 1978).
- [3] J. D. Anderson, Jr, *A History of Aerodynamics* (Cambridge University Press, Cambridge, 1997).
- [4] I. H. Abbott and A. E. Von Doenham, *Theory of Wing Sections* (Dover, New York, 1959).
- [5] J. Moran, *An Introduction to Theoretical and Computational Aerodynamics* (John Wiley, 1984).